LRS-1: A New Delaminated Phyllosilicate Material with High Acidity

Bachar Zebib, Jean-François Lambert,* Juliette Blanchard, and Michèle Breysse

Laboratoire de Réactivité de Surface (UMR 7609 CNRS), Université Pierre et Marie Curie, 4, Place Jussieu, 75252 Paris Cedex 05, France

Received March 24, 2005. Revised Manuscript Received July 1, 2005

Well-crystallized samples of the phyllosilicate magadiite have been synthesized in their sodic form, both purely silicic and with an Al/Si ratio of 30. They have been delaminated by a procedure consisting of $CTMA^+$ swelling in the presence of TPAOH, sonication, and calcination at 700 °C to remove the organics and characterized by XRD, ^{27}Al, and ^{29}Si NMR, IR, TEM, and SEM, and N_2 physisorption after the successive steps of this procedure. The final delaminated solids, consisting of crumpled sheets, exhibit a high (500−510 m^2/g), mostly external surface area. While ^{29}Si NMR indicated some loss of structural order, IR suggested the preservation of a typical feature of the magadiite sheets, namely, five-membered (TO_4) rings. The acidity of the delaminated Al-containing material was evaluated by low-temperature CO adsorption. This technique revealed strong Brönsted acidic centers, whose behavior was similar to that of Si−OH−Al bridging hydroxyls in pentasil zeolites. Finally, the catalytic activity was evaluated for the test reaction of cumene cracking and shown to be much higher than that of a reference silica alumina. These results make delaminated magadiite an attractive candidate for use as a novel acid catalyst or catalytic support.

Introduction

Successful cracking of hydrocarbon molecules necessitates strong acidic centers, and zeolites are, in this regard, better cracking catalysts than amorphous silica−alumina. However, the cracking of bulky molecule is still hindered by the small pore size of zeolite cavities, and this despite the work devoted during the past decades to the synthesis of zeolites with larger pore aperture. Ten years ago, when mesoporous MCM-41 materials were discovered, much hope was placed in their use as cracking catalysts because their large pore size could allow the cracking of larger molecules. However, it was rapidly clear that, whatever the synthesis procedure, their acidity was closer to amorphous silica−aluminas than to zeolites. More recently, syntheses of materials combining the acidity of zeolite and the porosity of organized mesoporous materials have been reported, but the true composition of the resulting catalyst, either a mixture of zeolite and mesoporous material or truly a mesoporous material with zeolite-like walls, is still questioned.

Meanwhile, alternative materials presenting acidity in open porosity have been tested. The starting materials used for the preparation of these new supports are aluminosilicates, including clays, with lamellar structure. They consist of extended two-dimensional layers, normally stacked up in "tactoids". In their native form, most of the layer surface is inaccessible due to this stacking. However, it has long been known that lamellar structures can be delaminated or exfoliated to form "house-of-cards" structures,[1,2] exhibiting high mesoporosity and/or external surface. This procedure, originally applied to clay materials, has recently been generalized to lamellar precursors of zeolitic structures, to yield the so-called "ITQ" phases (including ITQ-2, ITQ-6, and ITQ-18[3−9]) while closely related phases were obtained by pillaring.[10] Less attention has been paid to the application of this procedure to naturally occurring phyllosilicates such as magadiite and kenyaite, which are interesting candidates due to their high layer thickness and subsequent rigidity, although the first successful attempts to delaminate these materials were reported several years before the synthesis of ITQ materials.[11]

In the present article, we report (i) the successful delamination of magadiite to yield supports with high, mostly external surface area (500−600 m^2/g) consisting of separate layers that retain the basic connectivity of the starting materials, (ii) the introduction of substitutional Al in such materials, and (iii) the demonstration of a high acid catalytic

* Corresponding author. E-mail: lambert@ccr.jussieu.fr.

(1) Hofmann, U.; Fahn, R.; Weiss, A. *Kolloid-Z.* **1957**, *151,* 97.
(2) Occelli, M. L.; Landau, S. D.; Pinnavaia, T. J. *J. Catal.* **1984**, *90*, 256.
(3) Corma, A.; Fornes, V.; Guil, J. M.; Pergher, S.; Maesen, T. L. M.; Buglass, J. G. *Microporous Mesoporous Mater.* **2000**, *38*, 301.
(4) Corma, A.; Diaz, U.; Domine, M. E.; Fornés, V. *J. Am. Chem. Soc.* **2000**, *122*, 2804.
(5) Corma, A.; Fornés, V.; Sales Galletero, M.; García, H.; Gómez-García, C. J. *Phys. Chem. Chem. Phys.* **2001**, *3*.
(6) Corma, A.; Fornés, V.; Jordá, J. L.; Rey, F.; Fernandez-Lafuente, R.; Guisan, J. M.; Mateo, C. *Chem. Commun.* **2001**, *3*, 419.
(7) Corma, A.; Fornés, V.; Díaz, U. *Chem. Commun.* **2001**, 2642.
(8) Galletero, M. S.; Corma, A.; Ferrer, B.; Fornés, V.; García, H. *J. Phys. Chem. B* **2003**, *107*, 1135.
(9) Onida, B.; Borello, L.; Bonelli, B.; Geobaldo, F.; Garrone, E. *J. Catal.* **2003**, *2*, 191.
(10) He, Y. J.; Nivarthy, G. S.; Eder, F.; Seshan, K.; Lercher, J. A. *Microporous Mesoporous Mater.* **1998**, *25*, 207.
(11) Shih, S. S.; Vartuli, J. C. Catalyst comprising a hydrogenation metal and a delaminated layered silicate U.S. Patent 5,236,882, 1993; 7 pp.

10.1021/cm050643j CCC: $33.50
Published on Web 12/06/2005

activity for cumene cracking, comparable with the best zeolitic supports available.

Rather similar materials have been obtained starting from kenyaite phyllosilicates. Their comparison with magadiite-derived materials will be the object of a later publication.

Experimental Section

Na^+-Magadiite. Na^+-magadiite, with a formula of $Na_2Si_{14}O_{29}\cdot nH_2O$, was synthesized according to published methods.[12−14] The starting mixture was composed of $SiO_2/NaOH/H_2O$ with molar ratios of 9/2/75; the hydrothermal synthesis was carried out at 150 °C for 72 h, with stirring. The source of silica employed was a Ludox suspension (HS-40). The solid product was washed with deionized water and air-dried at room temperature.

Introduction of Al Substitution in the Magadiite Layers. This procedure was somewhat modified from refs 15 and 16. Al was introduced into the hydrothermal synthesis mixture as AlOOH (Aldrich), and the aging time was 10 days; other synthesis parameters were not modified. We used starting atomic ratios corresponding to Si/Al: 45 or 30. Elementary analysis (Centre d'Analyse du CNRS, Vernaison) indicated that at least 90% of the aluminum in the synthesis medium was incorporated into the solid phase. Therefore, we will refer to the Al-containing materials through the Si/Al ratio in the starting mixture, which is quite close to the actual ratio in the solid phase.

Swelling. Na^+-magadiite is easily intercalated by quaternary alkylammoniums.[17,18] The cation exchange reaction can be written as

$$Na_2Si_{14}O_{29}\cdot nH_2O + xR_4N^+ \rightarrow (R_4N)_xNa_{2-x}Si_{14}O_{29}\cdot zH_2O + xNa^+ + (n-z)H_2O \qquad [n = 9-11]$$

To swell the magadiite, 1 g of Na^+-magadiite was suspended in 4 g of distilled water. To this suspension were added 19.4 g of a hexadecyltrimethylammonium bromide solution (CTMABr, 29%) and 6.1 g of tetrapropylammonium hydroxide solution (TPAOH, 40%). The resulting suspension was heated to 85 °C for 16 h. This swelling procedure was repeated several times; the effect of varying the number of swellings will be commented on in a later publication.

Delamination. Delamination is a procedure that aims at the separation and loss of coherence between the layers of a lamellar material. Magadiite samples were delaminated by applying a procedure rather similar to that used by Corma et al. in the synthesis of ITQ materials: CTMA-intercalated magadiites were sonicated in an ultrasound bath for 1 h at 50 °C. The solid phase was dried and then calcined at 700 °C for 3 h.

In this article, we will compare the properties of delaminated silicic magadiite and delaminated Al-containing magadiite (corresponding to an initial Si/Al ratio = 30): the latter material will be called LRS-1.

Characterization. *X-ray Diffraction.* X-ray powder diffraction measurements were carried out on a Siemens D500 diffractometer (Cu Kα radiation, graphite monochromator) operating with a voltage of 30 kV. Diffractograms were recorded between 1.5° and 40° 2θ with a step of 0.02° 2θ.

Solid-State NMR. ^{29}Si and ^{27}Al MAS NMR spectra were obtained on an AV400 spectrometer (Bruker) with a sampling frequency of 79.4 MHz (^{29}Si) or 104.2 MHz (^{27}Al). For ^{29}Si NMR, the samples were placed in a rotor with a diameter of 7 mm, with a pulse width of 2 μs ($\pi/2$), a pulse delay of 20 or 60 s, and a spin rate of 4 kHz. For ^{27}Al NMR, a 4 mm rotor was used, with a pulse width of 0.5 μs ($\pi/6$), a pulse delay of 0.2 s, and a spin rate of 10 kHz.

Surface Area and Porosity. Nitrogen adsorption−desorption isotherms at 77 K were obtained using an ASAP model 2010 (Micromeritics) automated analyzer. The samples were outgassed at 150 °C overnight under a residual pressure of 1 Pa. The total surface area was determined using the BET method; mesoporous and external surfaces were evaluated from t-plots.

FTIR Spectroscopy and Probe Molecules Adsorption. IR spectra were recorded on a Bruker VECTOR 22 FT-IR spectrometer equipped with a DTGS detector, with a 4 cm^{-1} resolution. The samples were diluted in KBr pellets and recorded in the transmission mode. For CO adsorption experiments, we used a special cell that could be cooled by liquid-nitrogen-containing jackets. Self-supported pellets were pretreated under vacuum (10^{-3} Torr) for 2 h at 573 K. Adsorption was carried out at a temperature close to that of liquid nitrogen (77 K), raising the pressure stepwise in increments of 2−5 Torr. The final pressure after the last increment was about 2.5 Torr.

Electronic Microscopy. Transmission electron microscopy (TEM) was performed on a transmission electron microscope JEOL 100 CXII.

Catalytic Activity Measurements. Cumene cracking was carried out in a fixed-bed microreactor under atmospheric pressure at 573 K. The cumene (Aldrich, 99%) partial pressure was kept constant at 733 Pa. The flow rate of N_2 was 50 mL/min and the amount of catalyst was 50 mg. The reaction products were separated and identified on-line using a Perichrom gas chromatograph with a packed column The only observed products were propene and benzene (in particular, no α-methylstyrene, produced by dehydrogenation on Lewis sites, was observed). Prior to the activity measurement, each catalyst was pretreated in situ in N_2 (30 mL/min) at 773 K for 2 h (2 K/min).

Results and Discussion

Characterization of Al-Free and Al-Containing Materials throughout the Synthesis Procedure. The X-ray diffraction patterns of the starting material as well as those recorded after each step of the delamination procedure are given in Figure 1. The diffractogram of the starting silicic Na-magadiite (Figure 1a) has a strong peak at 15.7 Å, as compared to 15.6 Å reported in the literature for the d_{001} of the two water layers form.[19] It exhibits many other peaks corresponding to d_{hkl} with k and/or $l \neq 0$, indicating well-ordered Na-magadiite crystallites.

After swelling with CTMABr (Figure 1b), d_{001} has increased to 30.2 Å, indicating ($CTMA^+$) intercalation in the interlayer space (a d_{001} value of 30.0 Å was reported by Lagaly et al. for CTMA-swollen magadiite[17]). The peak observed at 15.0 Å could be due to a residual amount of unintercalated material, but more likely corresponds to the second order (d_{002}) of the main reflection of the intercalated form. Most other peaks of the magadiite layers seem to have undergone coalescence into broad bands, a phenomenon

(12) Beneke, K.; Lagaly, G. *Am. Mineral.* **1975**, *60*, 642.
(13) Fletcher, R. A.; Bibby, D. M. *Clays Clay Min.* **1987**, *35*, 318.
(14) Kikuta, K.; Ohta, K.; Takagi, K. *Chem. Mater.* **2002**, *14*, 3123.
(15) Schwieger, W.; Pohl, K.; Brenn, U.; Fyfe, C. A.; Grondey, H.; Fu, G.; Kokotailo, G. T. *Stud. Surf. Sci. Catal.* **1995**, *94*, 47.
(16) Pál-Borbély, G.; Auroux, A. *Stud. Surf. Sci. Catal.* **1995**, *94*, 55.
(17) Lagaly, G.; Beneke, K.; Weiss, A. *Am. Mineral.* **1975**, *60*, 642.
(18) Brenn, U.; Schwieger, W.; Wuttig, K. *Colloid Polym. Sci.* **1999**, *277*, 394.
(19) Eypert-Blaison, C.; Michot, L. J.; Humbert, B.; Pelletier, M.; Villiéras, F.; d'Espinose de la Caillerie, J.-B. *J. Phys. Chem. B* **2002**, *106*, 730.

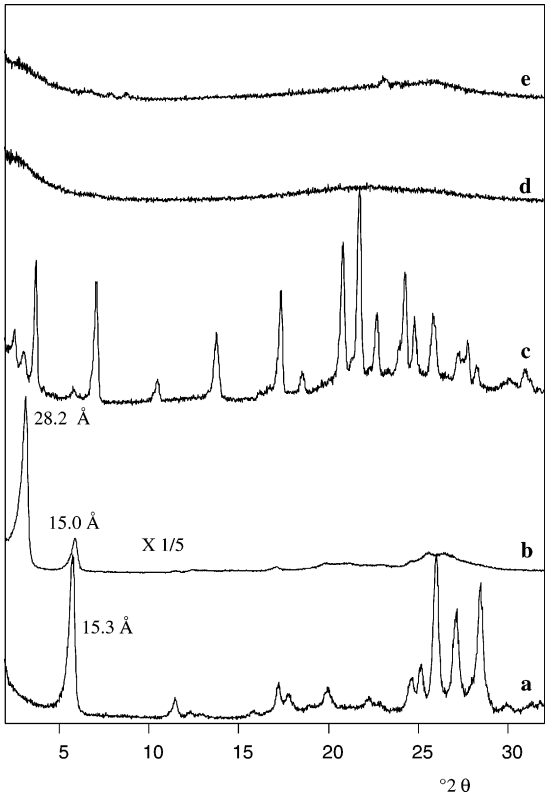

Figure 1. DRX of (a) silicic Na-magadiite, (b) same, after $CTMA^+$ swelling, (c) same, after sonication and drying, (d) same after calcination (delaminated silicic magadiite); (e) Al-substituted magadiite (Si/Al = 30), after the final step of calcination (sample LRS-1).

reminiscent of the turbostratic stackings observed for many clay minerals (*hkl* peaks with common values of *h*, *k*, and variable *l* are observed as a broad "*hk*" band).

After sonication and drying (Figure 1c), many sharp diffraction peaks are observed. However, most of these peaks may also be observed in the diffractogram of pure CTMABr deposited on a glass slide, and therefore they are assigned to a CTMABr phase separated from the inorganic material.

Finally, when the organic material has been eliminated by calcination, the resulting material is essentially X-ray amorphous (Figure 1d), and in particular the d_{00l} peaks indicative of the stacking of the silicate layers have been lost.

Very similar evolutions are observed when the same procedure is applied to an Al-substituted magadiite (Si/Al = 30). Only the final stage (after calcination) is shown here in Figure 1e: the resulting material (LRS-1) is also X-ray amorphous.

Techniques sensitive to short-range order, such as ^{29}Si NMR and IR spectroscopies, can shed some light on the nature of these amorphous materials. Figure 2 compares the ^{29}Si NMR spectra at various stages of the preparation. The starting silicic Na-magadiite (Figure 2a) exhibits the pattern that has been previously observed,[19−21] with three peaks in the Q^4 region at −109.2, −111.1, and −113.6 ppm and one in the Q^3 region at −99.2 ppm. Swelling causes the peaks to broaden and shift slightly (not shown), while keeping the

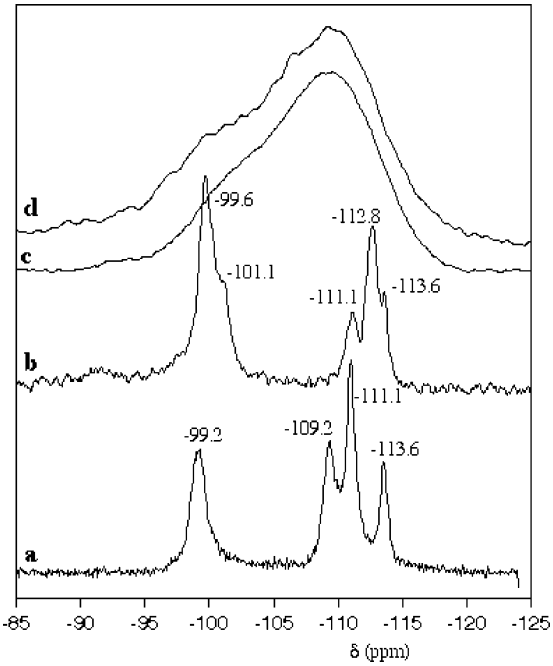

Figure 2. ^{29}Si MAS NMR of (a) silicic Na-magadiite, (b) same, after swelling, sonication, and drying, (c), same after final calcination (delaminated silicic magadiite); (d) sample LRS-1.

same overall pattern and relative intensities as in the starting Na-magadiite. Such shifts are typical of changes in local constraints inducing small modifications in the Si−O−Si angles, and many such examples have been reported in zeolites:[22−25] there is little doubt that the basic structure of the silicic sheets is conserved. Sonication and drying cause further transformation of the ^{29}Si NMR spectrum (Figure 2 b): three peaks in the Q^4 region at −111.1, −112.8, and −113.6 ppm and one peak in the Q^3 region at −99.6 ppm seem closely related to those of the starting magadiite, but we also observe an additional Q^3 peak at −101.1 ppm, possibly due to different compensating cations (Na^+, $CTMA^+$) in the vicinity of the tetrahedra pointing into the gallery.

After the final calcination step, on the other hand (Figure 2c), the individual signals of magadiite sheets are no longer individually recognizable, although one can still clearly discriminate between Q^3 and Q^4 components, in approximately the same intensity ratio as in the starting material.

Once again, the evolution of Al-substituted magadiites during the successive treatments is very similar. The starting ^{29}Si NMR spectrum is less well-resolved, probably due to different local environments for the same crystallographic site (Q^4-*n*Al, or Q^3-*n*Al, with different values for *n*, the number of Al neighbors). The ^{29}Si spectrum of sample LRS-1 (Si/Al = 30, after the final step of calcination) is shown in Figure 2d and is all but superimposable on that of the Al-free delaminated material.

It is important to note that ^{27}Al NMR (Figure 3) of Al-containing materials shows a single peak at +51.6 ppm, i.e.,

(20) Garcés, J. M.; Rocke, S. C.; Crowder, C. E.; Hasha, D. L. *Clays Clay Miner.* **1988**, *36*, 409.
(21) Fyfe, C. A.; Skibsted, J.; Schwieger, W. *Inorg. Chem.* **2001**, *40*, 5906.
(22) Rees, L. *Nature* **1983**, *303*, 204.
(23) Engelhardt, G.; Luger, S.; Buhl, J. C.; Felsche, J. *Zeolites* **1989**, *9*, 182.
(24) Vomscheid, R.; Briend, M.; Peltre, M. J.; Massiani, P.; Man, P. P.; Barthomeuf, D. *Chem. Commun.* **1993**, 544.
(25) Hunger, M.; Horvath, T. *Ber. Bunsen-Ges.* **1995**, *99*, 1316.

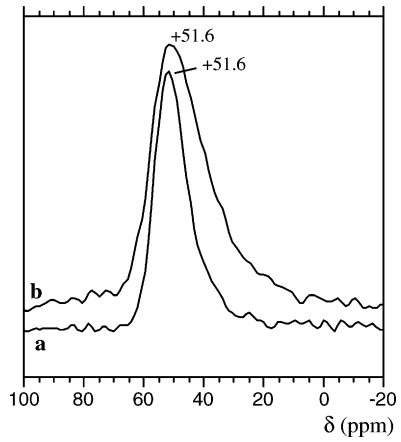

Figure 3. ^{27}Al MAS NMR (central transition) of (a) starting Al-substituted magadiite (Si/Al = 30) and (b) sample LRS-1.

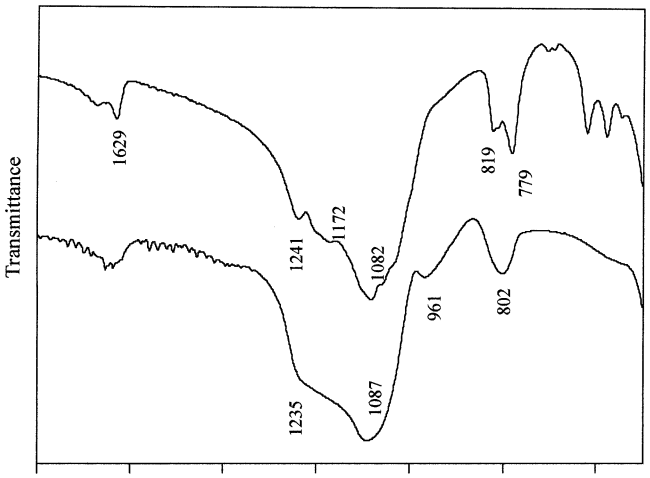

Figure 4. Middle IR transmission spectra of (a) silicic Na-magadiite and (b) same, after swelling, sonication, drying, and calcination (delaminated silicic magadiite).

in the region of tetrahedral Al, without any octahedral Al being present. This conclusion is valid both before (Figure 3a) and after (Figure 3b) the delamination procedure. Therefore, we believe that almost all of the Al is in a substitutional position in the magadiite layers.

The middle IR spectra of the starting silicic Na-magadiite (Figure 4a) and its calcined delaminated counterpart (Figure 4b) exhibit some bands in the 1800−500 cm^{-1} range where lattice vibrations are found. The spectrum of Na-magadiite is identical to those published in previous studies.[20,26] The most intense bands (at 1082 and 1052 cm^{-1} in Na-magadiite, broad band around 1087 cm^{-1} in the delaminated material) are ν_{as} Si−O−Si asymmetric stretching vibrations. Two bands at 779 and 819 cm^{-1} in Na-magadiite are probably $\nu_{symSi-O-Si}$; in the calcined material, they are replaced by a broad signal at 802 cm^{-1}. Of particular interest is the cluster of bands at 1172, 1208, and 1241 cm^{-1}. Bands around 1240 cm^{-1} have been specifically assigned to Si−O−Si stretching modes of five-membered rings in the magadiite structure,[20,26] by analogy to the bands found in the same region for pentasil zeolites such as ZSM-5 or ZSM-11. Figure 4b indicates that a well-defined shoulder is still present at 1235 cm^{-1} in the calcined material. This may be construed as evidence for the existence of five-membered rings in the calcined material, although it is not fully diagnostic since an LO mode of $\nu_{sym\ Si-O-Si}$ has been reported in the same region.[27] In the OH stretching region (not shown here), a strong, sharp band at 3748 cm^{-1}, attributable to silanol groups, is apparent for calcined, delaminated materials. In addition, the Al-containing delaminated support LRS-1 also shows a broad shoulder around 3615 cm^{-1}, i.e., at a wavenumber value close to that observed for bridging Si−OH−Al in zeolites such as H-ZSM5 (3616 cm^{-1}) so that a similar assignment seems to be in order (not shown, but see Figure 7).

In summary, both ^{29}Si NMR and IR data could be explained by postulating that the basic structure of magadiite layers is conserved upon delamination, but with a strong loss of local ordering due to deformation of the layer and local corrosion. However, it may still be argued at this point that the spectroscopic signatures of the delaminated all-Si material are not very different from those of amorphous silicas such as aerosils (in contrast, LRS-1 is significantly different from average silico-aluminas since it lacks octahedral Al).

More definite evidence for a specific individuality of delaminated materials can be found when examining its texture by electron microscopy. Figure 5 shows TEM micrographs of the starting silicic Na-magadiite and the calcined delaminated material. Na-magadiite appears as stackings of well-defined rectangular layers with sizes in the 100 nm to 1 μm range. The calcined material still shows some particles of rectangular morphology, but they do not appear as neat stackings anymore. They are partly broken up and appear to be curled or crumpled when observed with the correct orientation. The appearance of the particles is quite distinct from that of an amorphous silica. Scanning electron microscopy has also confirmed the crumpled sheets morphology.

Figure 6 shows the N_2 adsorption−desorption isotherms of the starting Na-magadiite, the delaminated silicic magadiite, and sample LRS-1; Table 1 summarizes the main results of isotherm analysis. The original material shows a small, mostly external surface area, comparable to that of a typical clay mineral. After delamination and calcination, the surface area increases by over an order of magnitude (to 513 m^2/g for LRS-1). Some mesoporosity is developed, as evidenced by an H3-type hysteresis loop, generally attributed to slit-shaped pores between platelike particles forming loose aggregates.[28] However, most of the surface is external and/or mesoporous (over 80%) and should therefore be easily accessible. Taken together, the N_2 physisorption and TEM results strongly suggest that the procedure we applied has indeed resulted in delamination, i.e., in a loosening of the coherence between magadiite layers while mostly preserving the connectivity of each individual layer.

Evidence for Strong Acidity in the Al-Containing Material LRS-1. We have evaluated the potential of our materials as acidic catalysts by a combination of probe

(26) Huang, Y.; Jiang, Z.; Schwieger, W. *Chem. Mater.* **1999**, *11*, 1210.

(27) Burneau, A.; Gallas, J.-P. 3A. Vibrational Spectroscopies. In *The surface properties of silicas*; Legrand, A. P., Ed.; J. Wiley & Sons: Chichester, 1998; p 147.

(28) Sing, K. S. W.; Everett, D. H.; Haul, R. A. W.; Moscou, L.; Pierotti, R. A.; Rouquerol, J.; Siemieniewska, T. *Pure Appl. Chem.* **1985**, *57*, 603.

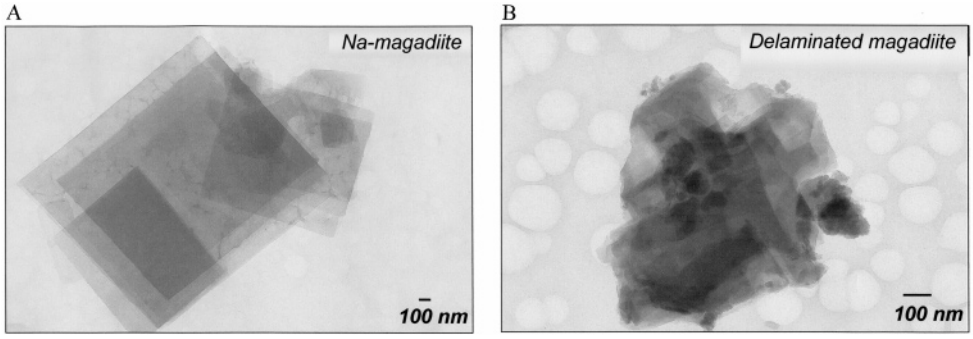

Figure 5. TEM micrographs of (A) starting silicic Na-magadiite and (B) sample LRS-1.

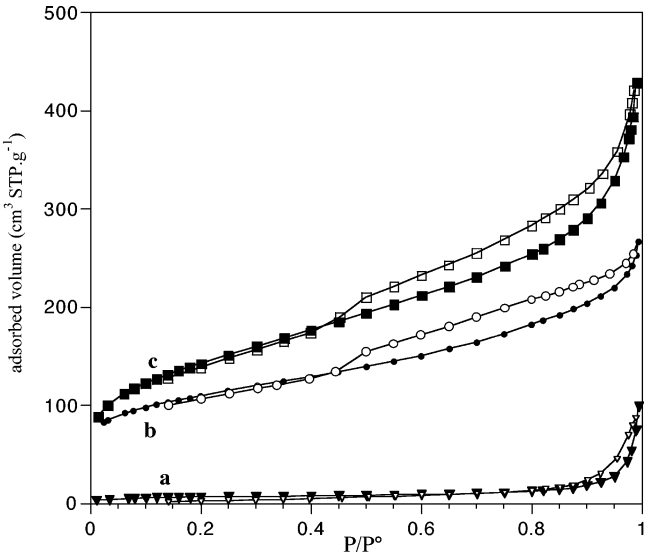

Figure 6. N_2 adsorption−desorption isotherms (77 K) on (a) starting silicic Na-magadiite, (b) delaminated silicic magadiite, and (c) sample LRS-1.

Table 1. Main Parameters Derived from N_2 Physisorption

sample	surface area (m^2/g)	external surface (m^2/g)	pore volume (mL/ g)	average pore diameter (Å)
silicic Na^+-magadiite	24	23 (96%)	0.05	(110)
delaminated silicic magadiite	500	340 (68%)	0.21	29
LRS-1 (delaminated magadiite, Si/Al = 30)	513	310 (60%)	0.25	30

molecules adsorption and test reactions. CO was used as a probe molecule since it is a weakly basic molecule that specifically combines with sufficiently acidic centers (of both Lewis and Brönsted types) and is rather easily monitored by IR spectroscopy in the transmission mode.

Figure 7A shows the IR difference spectra in the CO stretching region after adsorption of several successive carbon monoxide pulses (the final pressure after equilibration of the last pulse was 2.6 Torr). The first CO dose causes the appearance of two bands at 2228 and 2176 cm^{-1}, i.e., blue-shifted with respect to gas-phase carbon monoxide. The first one immediately saturates (indicative of a high CO/surface affinity) while the second one keeps growing asymptotically, without significant displacement (possible Langmuir-type behavior). At higher pressures, a second band starts growing at 2158 cm^{-1} and then a third one at 2139 cm^{-1}.

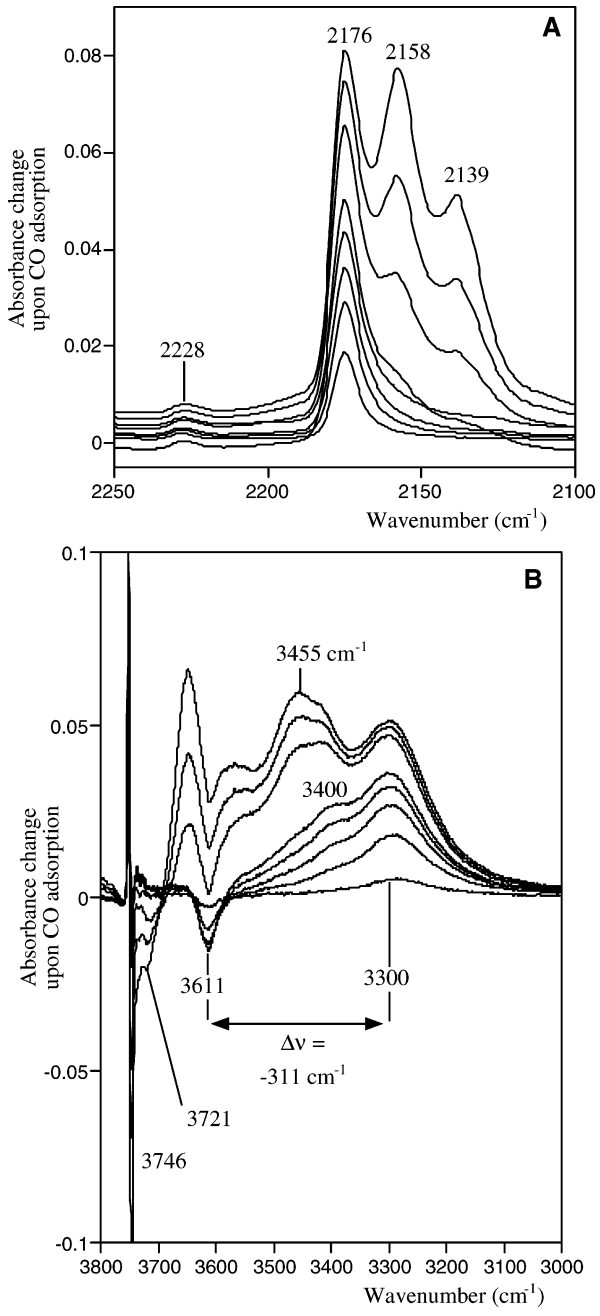

Figure 7. Middle IR transmission spectra after CO adsorption on material LRS-1, shown for several successive CO doses. (A) CO stretching region; (B) OH stretching region (difference spectrum with original LRS-1).

In parallel, significant modifications become obvious in the OH stretching region. They are shown in Figure 7B, as

difference spectra corrected for the adsorption of the sample unexposed to CO. The first doses cause an immediate decrease of the 3611 cm^{-1} shoulder accompanied by the growth of a broad and rather intense band at 3300 cm^{-1}. At intermediate pressures, a second, probably composite band appears in the 3460−3400 cm^{-1} region, with a final absorption maximum at 3455 cm^{-1}. In a third step, the absorbance starts increasing in the 3650−3550 cm^{-1} region (with the 3611 cm^{-1} dip still visible), while the main band at 3748 cm^{-1} decreases.

The interpretation of these data is rather straightforward if we compare them to the body of available evidence on zeolitic materials. The band at 2228 cm^{-1} is attributable to CO adsorbed on strong Lewis acidic sites:[29] in our samples, they are present in very low amounts. This was expected since the samples contain very little octahedral Al (if any).

The band at 2176 cm^{-1} is characteristic of CO H-bonded to strong Brönsted acidic centers, which are obviously much more frequent. The evolution of the OH stretching region indicates that these centers are associated with the bridging hydroxyls (Si−OH−Al) adsorbing at 3611 cm^{-1} in the starting material; the formation of an H-bond with CO weakens the O−H vibrator, which undergoes a red shift ($\Delta\nu_{OH}$) of −311 cm^{-1}. These figures can be compared with those obtained for CO adsorption on strongly acidic zeolites: on H-ZSM5, adsorbed CO is observed at 2176 cm^{-1} and causes a −310 cm^{-1} shift of the OH stretching of bridging hydroxyls.[30] The similarity is obvious. The correspondence is not so good with other acidic zeolitic materials, making it likely that ZSM5 and LRS1 share some structural features.

After the third CO pulse, a new OH stretching band appears at about 3400 cm^{-1} while the only CO stretching band observable is still at 2176 cm^{-1}, suggesting the existence of another kind of strongly acidic OH centers. However, it is unclear whether these centers are terminal silanols or bridging Si−OH−Al, and therefore estimates of the acidity based on $\Delta\nu_{OH}$ are not possible, especially since a new component at 3455 cm^{-1} becomes apparent later on.

In later steps, a CO stretching band appears at 2158 cm^{-1}. At the same time, an increase in the adsorption in the 3580−3620 cm^{-1} range becomes apparent. It is difficult to locate the maximum in this feature, but it lies at approximately −120 cm^{-1} with respect to the terminal silanols. These figures are comparable to those obtained on purely silicic materials such as MCM 41 (respectively ν_{CO} at 2156 cm^{-1} and $\Delta\nu_{OH}$ at −89 cm^{-1}) [31] or amorphous silica in silico-aluminas,[32] and therefore we are probably seeing CO adsorption on weakly acidic silanols.

Finally, the band at 2139 cm^{-1} is usually ascribed to "physisorbed" CO, either in multilayers or nonspecifically adsorbed through van der Waals interactions.

Several Al-containing phyllosilicate catalysts, including LRS-1, were then tested for activity in the cumene cracking reaction. Deactivation curves are provided in Figure 8, and steady-state activities are listed in Table 2.

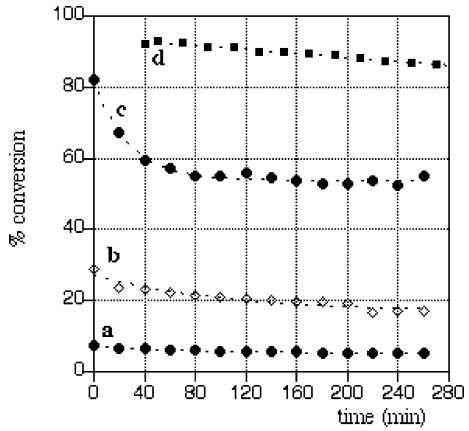

Figure 8. Cumene cracking deactivation curves for LRS-1 and some reference materials. (a) Al-substituted Na-magadiite; (b) silica alumina; (c) LRS-1; (d) H-BEA.

Table 2. Main Structural Parameters, and Cumene Cracking Activity, of LRS-1 as Compared to Several Reference Catalysts

sample	Si/Al ratio	surface area (m^2/g)	steady-state cumene conversion (%)
sample LRS-1	30	513	54
Al-substituted Na-magadiite	30	24	6
H-BEA	25	350	80
silica alumina	5	575	12

LRS-1 has a high steady-state activity for this acid-catalyzed reaction, of the same order of magnitude as that of H-BEA, one of the best catalysts reported so far. More significantly, it is significantly higher than the activity of a reference silico-alumina with comparable surface area. Delamination is necessary for this strong activity since the parent Na^+-containing magadiite only showed a weak level of cumene conversion. Finally, and not unexpectedly, preliminary experiments have shown that the level of Al substitution is a crucial parameter, with lower substitutions giving significantly less active catalysts. Regarding the rate of deactivation, sample LRS-1 deactivates quickly during the first hour on stream, after which it stabilizes and compares favorably with the best available zeolitic catalysts (Figure 8).

Conclusion

The initial justification for our study of magadiite- and kenyaite-derived materials was to obtain stable delaminates with a high proportion of accessible (external) surface area, which could then be tailored, e.g., for use in acidic catalysts by introduction of Al/Si substitutions in their lattice. Results available at this time indicate beyond reasonable doubt that high-surface silico-aluminic materials having quite original surface properties can indeed be obtained in this way: electron microscopy data, and especially the high cumene cracking activity, clearly show that LRS-1 is not a run-of-the-mill silico-alumina. If, as seems rather likely, the structural integrity of individual magadiite layers is mostly preserved throughout the delamination process, it could be that highly acidic surface centers are linked with the five-membered rings known to be present in the starting maga-

(29) Morterra, C.; Magnacca, G. *Catal. Today* **1996**, *27*, 497.
(30) Datka, J.; Gil, B.; Kawalek, M.; Staudte, B. *J. Mol. Struct.* **1999**, *511*−*512*, 133.
(31) Mori, T.; Kuroda, Y.; Yoshikawa, Y.; Nagao, M.; Kittaka, S. *Langmuir* **2002**, *18*, 1595.
(32) Daniell, W.; Schubert, U.; Glöckler, R.; Meyer, A.; Noweck, K.; Knözinger, H. *Appl. Catal. A* **2000**, *196*, 247.

diite: this feature would indeed be shared with another highly active catalyst, i.e., H-ZSM5.

The potential uses of such catalysts would be toward the cracking of bulky molecules that cannot penetrate the porous volume of a zeolitic framework. Current investigations are therefore directed at testing the activity of LRS-1 for such reactions, and optimizing preparation parameters, such as the Si/Al ratio, in this respect.

CM050643J